

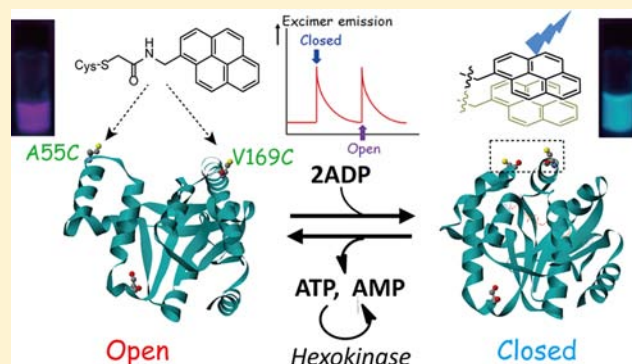
Reversible Switching of Fluorophore Property Based on Intrinsic Conformational Transition of Adenylate Kinase during Its Catalytic Cycle

Akira Fujii, Shun Hirota, and Takashi Matsuo*

Graduate School of Materials Science, Nara Institute of Science and Technology (NAIST), Ikoma, Nara 630-0192, Japan

Supporting Information

ABSTRACT: Adenylate kinase shows a conformational transition (OPEN and CLOSED forms) during substrate binding and product release to mediate the phosphoryl transfer between ADP and ATP/AMP. The protein motional characteristics will be useful to construct switching systems of fluorophore properties caused by the catalytic cycle of the enzyme. This paper demonstrates in situ reversible switching of a fluorophore property driven by the conformational transition of the enzyme. The pyrene-conjugated mutant adenylate kinase is able to switch the monomer/excimer emission property of pyrene on addition of ADP or P^1P^5 -di(adenosine-5')-pentaphosphate (Ap_5A , a transition state analog). The observation under the dilute condition ($\sim 0.1 \mu M$) indicates that the emission spectral change was caused by the motion of a protein molecule and not led by protein–protein interactions through π – π stacking of pyrene rings. The switching can be reversibly conducted by using hexokinase-coupling reaction. The fashion of the changes in emission intensities at various ligand concentrations is different between ADP, Mg^{2+} -bound ADP, and Mg^{2+} -bound Ap_5A . The emission property switching is repeatable by a sequential addition of a substrate in a one-pot process. It is proposed that the property of a synthetic molecule on the enzyme surface is switchable in response to the catalytic cycle of adenylate kinase.



INTRODUCTION

Naturally occurring proteins/enzymes show efficient catalytic activity and precise molecular recognition toward substrates or ligands because they have preorganized and highly ordered structures featured by α -helix, β -sheet, and their combination. Since these preset structures provide us with unique reaction environments, modification of proteins is attractive in the development of artificial proteins and biocatalysts.^{1–3}

In contrast, some proteins exhibit their intrinsic functions by rearrangement of the structures resulting from external stimuli (e.g., binding of a specific ligand to a protein matrix). For example, proteins responsible for signal transducing *in vivo* undergo domain-based structural changes,^{4,5} during which the distance between the two amino acids belonging to different domains is likely to change remarkably ($>10 \text{ \AA}$). When synthetic compounds with distance-dependent properties are, consequently, conjugated to these amino acid residues, the chemically modified proteins should be able to switch the property of the conjugated compounds by the structural change. In this work, we demonstrate a reversible and repeatable switching system of the property of fluorophores conjugated on the enzyme surface in response to the catalytic reaction of the enzyme with a large conformational transition. The strategy will be complementary to that using photochromic compounds such as azobenzene,^{6–8} because the equilibrium

between the two states can be controlled by the amounts of ligand molecules. Furthermore, protein-based systems may be extended to methods for monitoring enzymatic reactions in biological systems.

Expected functions switched by the structural dynamics of a protein include: size alteration of the protein, change in the spectrophotometric property of molecules attached on the surface of the proteins, and so on. As an example of size alteration, some size-changeable protein hydrogels have been reported.^{9–11} In the switching of the spectrophotometric properties, possible methods for detection of spectral changes are fluorescence quenching/enhancement of one fluorophore moiety by the another,^{12,13} energy transfer between the two fluorophores (e.g., FRET mechanism),^{14–16} and aggregation of introduced fluorophores.^{17,18} These phenomena originate from proximity or separation of the two fluorophore molecules and have been often used for investigation of bimolecular processes (i.e., protein–protein or protein–small molecule interactions). Investigations of protein motion and protein–small molecule interactions by using fluorophores and spin-labeled compounds have also been reported.¹⁹

Received: March 28, 2013

Revised: May 10, 2013

Published: May 29, 2013

When switching of the spectrophotometric properties is targeted using a single protein molecule, the problem to be considered is the competition with interprotein processes in several protein molecules.²⁰ To avoid this problem, one of the methods is to examine the property switching under dilute conditions, although the strategy causes the decrease in sensitivity. Furthermore, reversible switching, not one-way switching, provided by the protein motions is a more challenging subject. In this context, we paid attention to the conformational transition of adenylate kinase (Adk) from *E. coli* (denoted as "Adk_e") and examined *in situ* reversible switching of the emission properties of pyrene through the catalytic cycle of Adk_e (Figure 1).

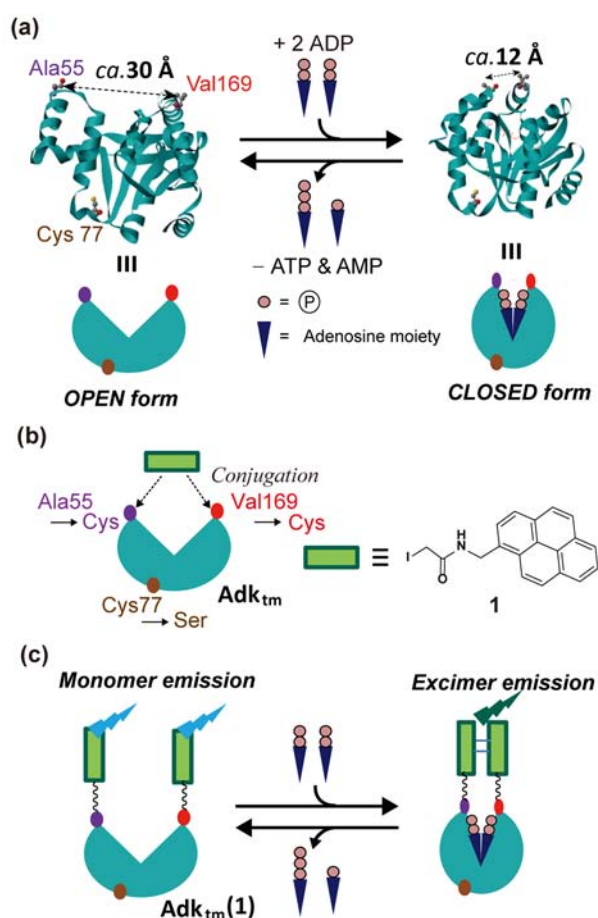


Figure 1. Protein-based switching system for pyrene emission property. (a) Conformational transition of adenylate kinase from *E. coli* (Adk_e) (PDB code: 4AKE for the OPEN form and 1AKE for the CLOSED form). (b) Mutation of Adk_e and conjugation of pyrene 1. (c) Switching of emission property by Adk_{tm}(1).

Adk (EC 2.7.4.3) is an enzyme related to cellular energy homeostasis, which is conserved in many kinds of organisms. The enzyme catalyzes the reversible phosphoryl transfer between adenine nucleotides ($2\text{ADP} \rightleftharpoons \text{ATP} + \text{AMP}$) in the presence of Mg^{2+} ,^{12,21–24} and undergoes the domain-based structural interconversion between the two structural states (OPEN and CLOSED forms, see Figure 1a) according to substrate-binding/product release.^{25,26} In the case of Adk_e, the distance between Ala55 and Val169 dramatically changes during the processes (ca. 30 Å in the OPEN form and ca. 12 Å in the CLOSED form).¹⁰

Pyrene has been known to show an emission band around 400 nm under dilute conditions (so-called “monomer emission”), whereas the emission band intensity decreases with the appearance of a new emission band in the longer wavelength region under concentrated conditions.²⁷ The new emission band is caused by excimer formation or π – π interactions between pyrene rings at the ground state. The change in the emission spectrum is possible under dilute conditions when two pyrene rings are set at the conformation-fused situations (e.g., a face-to-face covalent linkage²⁸ or inclusion in a narrow hydrophobic cavity^{29–31}). The character has often been used for sensing metal ions and biomolecule association.^{32–35} Evaluation of the distance between two amino acid residues in a helical moiety in a protein is also attempted by using the emission property of pyrene.³⁶ Consequently, pyrene is a good tool for investigating whether the fluorescence property can be exactly switched by the structural transition during the catalytic cycle of enzyme. In this context, we examined the conjugation of pyrene 1 to the position of Ala55 and Val169 in Adk_e to prepare a pyrene-conjugated Adk_e, Adk_{tm}(1), and attempted to observe the switching of the pyrene emission property by the Adk_e catalytic cycle.

EXPERIMENTAL SECTION

Materials. All commercially available materials were from conventional commercial sources and used as received unless otherwise noted. The pEAK91 plasmid coding the double mutant of Adk (A55C/C77S) was a gift from Prof. Elisha Haas (Bar-Ilan University, Israel). Designed primers were purchased from Invitrogen. A kit for plasmid extraction (QIAprep Spin Miniprep kit) was purchased from QIAGEN. KOD-plus-Mutagenesis Kit for inverse PCR was purchased from TOYOBO. Pyrene 1 was synthesized by the method described below. Hexokinase and glucose-6-phosphate dehydrogenase from baker’s yeast were purchased from Sigma as a mixed material (catalog code: H8629–500UN).

Instruments. ¹H NMR spectra were collected on a JEOL JNM-ECP400 spectrometer. MALDI-TOF-MS spectra were measured using a Bruker AutoFlex II mass spectrophotometer. ESI-MS analysis was carried out using a JEOL JMS-700 mass spectrometer. UV–vis spectra were recorded on a Shimadzu UV-2550 double beam spectrophotometer with a thermostatted cell holder. Protein purification was carried out using a BioRad Biologic Duoflow liquid chromatography system in a chromatochamber (4 °C). Emission spectra were recorded on a HITACHI F4500 fluorescence spectrophotometer. CD spectra were measured using a JEOL J-725 circular dichroism spectropolarimeter.

Synthesis of Pyrene 1. 1-Aminomethylpyrene hydrochloride (30 mg, 0.12 mmol) was suspended in 30 mL of 3 M NaOH_{aq} and extracted with CH_2Cl_2 . The organic phase was dried over Na_2SO_4 and the solvent was evaporated to yield 1-aminomethylpyrene as white solids (24 mg, yield 93%). In a 50-mL round-bottom flask, 1-aminomethylpyrene (17 mg, 0.074 mmol) and *N,N*-diisopropylethylamine (6.6 mg, 0.052 mmol) were dissolved in dry CH_2Cl_2 under a N_2 atmosphere. After the addition of *N*-iodoacetic succinimide (25 mg, 0.088 mmol) to the solution, the reaction mixture was stirred at room temperature for 2 h in the dark. The solvent was evaporated and the residue was subjected to silica gel column chromatography (eluent: CH_2Cl_2) to collect the first eluted fraction. Evaporation of solvent yielded pyrene 1 as white solids (23 mg, yield 78%). ¹H NMR (400 MHz, CDCl_3 , TMS) δ =

8.25–8.16 (m, 5H, pyrene), 8.11–7.98 (m, 4H, pyrene), 6.31 (s, 1H, NH), 5.19 (d, 2H, CH₂NH), 3.76 (s, 2H, CH₂I). ESI-HR-MS (direct, positive mode) calcd. for C₁₉H₁₄INO⁺ 399.0120; found 399.0121.

Expression of Adk_{tm}. The plasmid pEAK91 coding Adk_{tm} was derived from the plasmid coding the double mutant of Adk_c (A55C/C77S) by site-directed mutagenesis using inverse PCR method (Forward primer: ACGTTTACG-TACCGTCTCTTCCTGATC, Reverse primer: CTGTGTGAATACCATCAGATGACAGCA). HB101 *E. coli* (Novagen) transformed by the pEak91 plasmid was cultivated in LB media (5 mL) in the presence of ampicillin at 37 °C for 9 h. The culture was added to 2 L of LB medium and further cultivated at 37 °C for 16 h. After centrifugation, the resulting pellets were suspended in 50 mM Tris buffer (pH = 7.5), containing 0.1 M NaCl_{aq}. The expressed protein was extracted by freeze-and-thaw procedure, followed by sonication. The supernatant obtained by centrifugation was dialyzed against 50 mM Tris buffer (pH = 7.5) containing 1 mM TCEP (tris(2-carboxyethyl)phosphine) and concentrated by ultrafiltration. The resulting protein solution was passed through a DEAE sepharose column (GE healthcare) with elution of 50 mM Tris buffer (pH = 7.5) containing 1 mM TCEP. Next, the protein solution was absorbed in a BLUE sepharose column (GE healthcare) and washed with 50 mM Tris buffer (pH = 7.5) containing 1 mM TCEP. The protein was eluted by linear gradient of KCl (0–500 mM) in 50 mM Tris buffer (pH = 7.5) containing 1 mM TCEP. The second fraction containing Adk_{tm} (checked by SDS-PAGE) was collected and concentrated before being applied to a Sephadex G-75 gel column chromatography with elution of 50 mM Tris buffer (pH = 7.5) containing 1 mM TCEP. The protein solution was desalted by dialysis against water and lyophilized.

Conjugation of Pyrene 1 to Adk_{tm} (Preparation of Adk_{tm}(1)). Conjugation of **1** to Adk_{tm} was carried out in 50 mM HEPES (pH = 8.0) at 25 °C. After the addition of **1** (50 equiv) dissolved in DMSO to a buffer solution of the protein (DMSO 5% (v/v) in final), the mixture was gently stirred for 16 h in the dark. After centrifugation, the supernatant was dialyzed against 20 mM Tris buffer (pH = 8.0) and applied to a MonoQ column (GE healthcare) to separate from the unmodified and singly modified proteins. The second fraction containing Adk_{tm}(1) was collected and kept at –80 °C. Adk activity for Adk_{tm}(1) was confirmed by a hexokinase/glucose-6-phosphate dehydrogenase coupled reaction, where the absorbance at 340 nm derived from NADPH was monitored.³⁷

UV–vis and Fluorescence Measurements. All UV–vis and emission spectra were collected in a 1-cm quartz cell under the aerobic conditions. For measuring the emission spectra for ADP binding to Adk_{tm}(1) in the presence of Mg²⁺, the samples containing different ADP concentrations were independently prepared and spectra of each sample were rapidly collected immediately after addition of Mg²⁺ to avoid the conversion of ADP into ATP/AMP.

RESULTS AND DISCUSSION

Preparation and Characterization of Adk_c Conjugated with Pyrene 1 (Adk_{tm}(1)). Pyrene **1** was introduced into the Cys residues of the triple mutant of Adk_c (A55C/C77S/V169C, Adk_{tm})^{10,38} through thiolate nucleophilic attack to the iodoacetamide moiety (Figure 1b). The mutation at Cys77 is essential in avoiding the conjugation of **1** to this position. The X-ray crystallographic data of Adk_c indicate that Ala55 and

Val169 belong to different domains and are located on structurally rigid α -helices. Furthermore, a previous investigation using a series of Adk_c variants obtained by conversion of several amino acid residues into Cys suggested that these two amino acid residues are accessible for chemical modification, since their side chains are solvent-exposed.³⁸ Although the side chains of Ala55 and Val169 oppositely take orientations in the OPEN form, these are forced to take a face-to-face orientation in the CLOSED form. Consequently, the positions of Ala55 and Val169 will be suitable places for introduction of synthetic molecules to construct a function-switching system based on the protein structural change as depicted in Figure 1.

The pyrene-modified enzyme, Adk_{tm}(1), was successfully purified by anionic exchange column chromatography to remove the unmodified and the single-modified enzymes (Figure S1 of Supporting Information). The MALDI-TOF-MS measurement (Figure 2) detected a peak at $m/z = 24,149$,

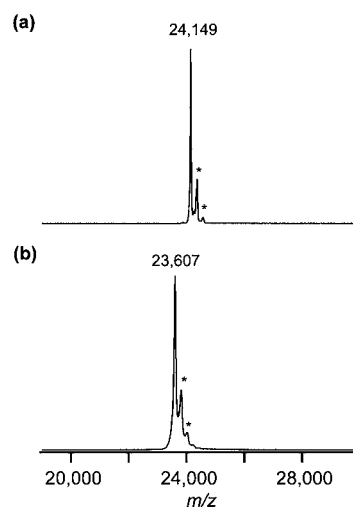


Figure 2. MALDI-MS spectra of Adk_{tm}(1) (Spectrum (a)) and the unmodified Adk_{tm} (Spectrum b). The peaks with asterisk (*) are assigned as matrix (sinapinic acid) adducts.

corresponding to the molecular weight of [Adk_{tm}(1) + H]⁺ ($M_w = 272$ for **1** – I[–]). The conjugation of two molecules of **1** to Adk_{tm} was confirmed. The CD spectra (Figure S2) indicate that the secondary structure of the enzyme is not significantly affected by the chemical modification. Judging from similar CD spectra for the unmodified and modified Adk_c, we can consider that the pyrene rings do not go into the inside of the protein, because the side chains of Cys55 and Cys169 will be solvent exposed (*vide supra*). If the pyrene rings are buried in the protein matrix, the α -helices including these amino acid residues would be significantly affected, resulting in the decrease of CD signal intensity. The phosphoryl transfer activity was retained for Adk_{tm}(1) (Figure S3), although a slight decrease in the activity was observed. This may be mainly caused by the increase in K_m value, and similar results have been reported for some mutant Adk_cs.¹²

UV–vis and CD Spectral Changes on Binding of Substrate/Transition State Analogue. At first, we attempted to observe the spectral changes on the binding of ADP or P¹P⁵-di(adenosine-5')pentaphosphate (Ap₅A), a transition state analogue for Adk (see the structure in Figure 3),¹⁰ to Adk_{tm}(1). Adk_c has two substrate-binding sites, which are located in the different domains: LID domain (the ATP-producing domain)

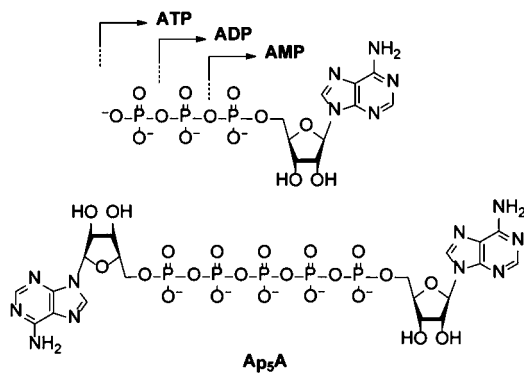


Figure 3. Structures of adenosine nucleotides and Ap₅A.

and AMP-bd domain (the AMP-producing domain), respectively.^{15,16,39} When ADP is substrate, two molecules of ADP bind to both sites (2:1 binding). In contrast, Ap₅A occupies the two sites with the 1:1 binding mode, because the compound possesses the two adenosine rings in its structure.

UV-vis and emission spectra of Adk_{tm}(1) are shown in Figure 4. The chemically modified enzyme has the distinct

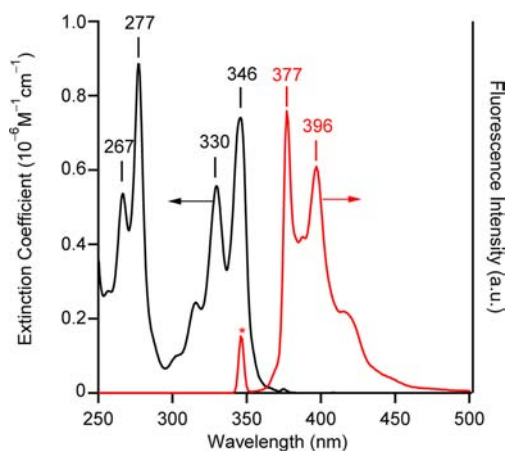


Figure 4. UV-vis (black line, left axis) and emission (red line, right axis) spectra of Adk_{tm}(1) in 50 mM Tris buffer (pH = 7.5). The emission spectrum was measured with excitation at 346 nm. The peak at 346 nm in the emission spectrum (with asterisk) originated from the scattering of excitation light.

absorption bands at 330–350 nm (black line), caused by the ¹L_a transition along the long axis in the pyrene ring.³¹ The spike peaks appearing at 377 and 396 nm in the emission spectrum (red line) are typical in the monomer emission of pyrene.¹⁴ These spectroscopic characteristics indicate no significant aggregation of the pyrene moieties in aqueous media. The consideration is based on the previously reported fact that the shape of the absorption spectrum at 330–350 nm becomes broad with low peak resolution in the presence of ground state interactions between pyrene rings.³¹

Figure 5 demonstrates the UV-vis and CD spectral changes on the addition of ADP or Ap₅A as a ligand. When the ligand was added to a protein solution, the absorbance of the ¹L_a absorption band decreased (Figure 5a). A similar finding has been reported for the pyrene dimer formation in a cyclodextrin cavity.³¹ The CD spectra (Figure 5b) of Adk_{tm}(1) in the presence of ADP or Ap₅A exhibited a dispersion-type signal around the maximum wavelength in the UV-vis spectra,

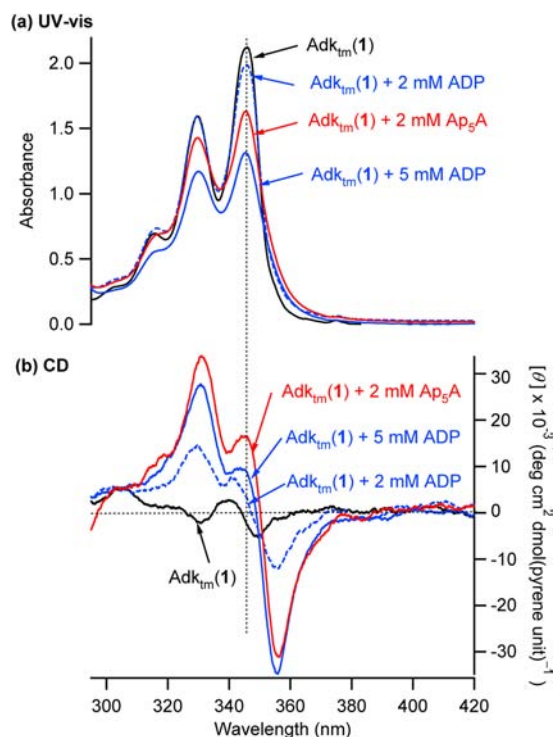


Figure 5. UV-vis and CD spectra of Adk_{tm}(1) (28 μM) in the absence and presence of ligand at 25 °C. (a) UV-vis spectra in 50 mM Tris buffer (pH = 7.5); (b) CD spectra in 10 mM potassium phosphate buffer (pH = 7.5).

whereas no distinct signal was observed in the protein-free system (the mixtures of the protein-free pyrene with ADP or Ap₅A (Figure S4)). Consequently, the appearance of the CD signals on the addition of ADP or Ap₅A is attributed to the encounter of the two pyrene moieties driven by the structural transition from the OPEN form to the CLOSED form. The CD signal sign is positive in the high-energy region and negative in the low-energy region. This is indicative of the left-handed chirality (*S*-helicity) in the complex.³¹ Ap₅A affects the UV-vis and CD spectra more strongly than ADP, suggesting that the conformational change becomes more significant in the transition state of the phosphoryl transfer process (*vide infra*).

Switching of Pyrene Emission Property on Binding of Substrate/Transition State Analogue. Next, we examined the switching of the emission property by ligand binding. On the addition of ADP to Adk_{tm}(1), the emission band around 400 nm distinctly decreased with generation of a new broad band around 485 nm (Figure 6). Similar spectral changes were also observed on the addition of Ap₅A (see Figure S5).⁴⁰ Since the excitation spectrum obtained with detection of the emission at 485 nm (Figure S6) is very similar to the absorption spectrum of Adk_{tm}(1), the new emission band is assignable as excimer emission, not the emission originating from the association at the ground state (so-called “ground state dimer”). Furthermore, the observed emission is not derived from the π - π interaction between pyrene-adenine rings, since no emission band around 485 nm was observed in the protein-free system (Figure S7).

The noticeable fact is that the pyrene excimer emission shown in Figure 6 was produced in a dilute solution of Adk_{tm}(1) (0.18 μM), whereas the excimer emission is only observable under highly concentrated conditions (>4 mM) without the protein (Figure S8). This indicates that the

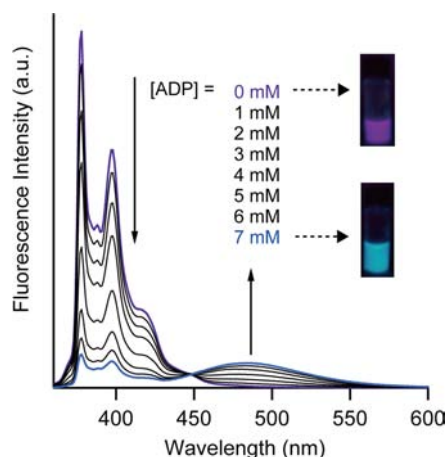


Figure 6. Emission spectral changes in titration by ADP for Adk_m(1) (0.18 μM) in 50 mM Tris-HCl, pH 7.5 at 25 °C. The purple and light blue spectra were taken at [ADP] = 0 mM and 7 mM, respectively. The pictures shown in inset were taken by irradiating the sample solution with a black-light lamp (365 nm). λ_{ex} = 346 nm.

appearance of the excimer emission band shown in Figures 6 and S5 is not derived from the interprotein dimerization but from the conformational change of a single molecule of the protein. In other words, switching of the pyrene emission property was successfully attained based on the conformational transition of Adk during substrate binding.

Figures 7 and 8 demonstrate the dependency of emission intensity on concentrations of Ap₅A and ADP, respectively. On

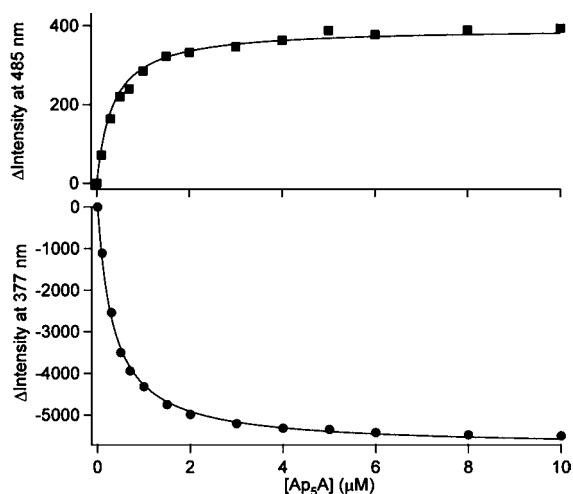


Figure 7. Dependency of emission intensities at 377 nm (monomer emission) and 485 nm (excimer emission) on concentrations of Ap₅A. [Adk_m(1)] = 0.18 μM; [MgCl₂] = 5 mM; 50 mM Tris-HCl, pH 7.5 at 25 °C. The solid lines are drawn based on the 1:1 binding model ($K = (3.6 \pm 0.1) \times 10^6 \text{ M}^{-1}$).

the addition of Ap₅A in the presence of Mg²⁺ (existed as Mg²⁺-bound form, denoted as Mg²⁺•Ap₅A), the emission intensities can be analyzed by the 1:1 binding model (Figure 7). This fact agrees with the binding fashion of Ap₅A to Adk (*vide supra*). The binding constant is evaluated to be $(3.6 \pm 0.1) \times 10^6 \text{ M}^{-1}$, which is similar to the previously reported value for the native Adk.¹⁹ This finding also supports our idea that the observed increase in the excimer emission stems from the conformational change caused by the Ap₅A binding.

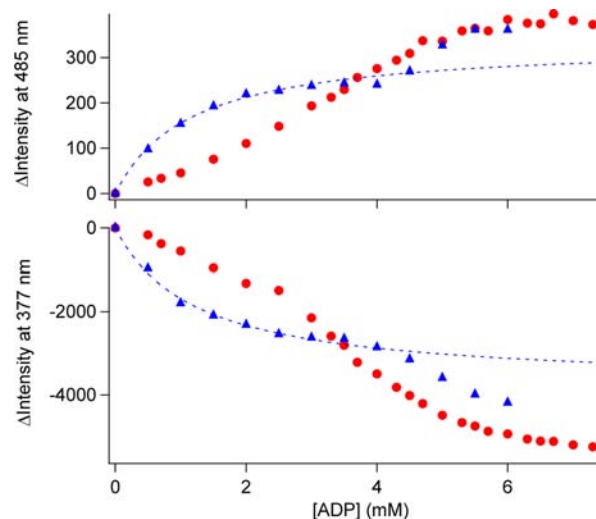


Figure 8. Dependency of emission intensities at 377 nm (monomer emission) and 485 nm (excimer emission) on concentrations of ADP in the absence of Mg²⁺ (red circles) and presence of Mg²⁺ (blue triangles). [Adk_m(1)] = 0.18 μM; [MgCl₂] = 0 or 10 mM; 50 mM Tris-HCl, pH 7.5 at 25 °C. The dotted lines on the data taken in the presence of Mg²⁺ are drawn by the 1:1 binding model ($K = (4.2 \pm 0.5) \times 10^3 \text{ M}^{-1}$) for the low concentration region (<2.5 mM). The emission intensities in the presence of Mg²⁺ were measured independently for each sample immediately after addition of the defined concentration of ADP to an enzyme solution.

In the case of ADP binding (Figure 8), larger concentrations of the ligand were required to clearly observe the spectral change, compared with Ap₅A binding. One of the possible reasons is that enzymes undergoing significant conformational change generally favor binding of a transition state analogue rather than a substrate, as proposed in “induced-fit” theory.⁴¹

Furthermore, the fashion of emission intensity changes are also different between the absence and presence of Mg²⁺ (the fluorescence spectra in the presence of Mg²⁺ were collected by rapid scanning immediately after addition of a defined concentration of ADP to the enzyme solution, which is essential for avoiding the conversion of ADP into ATP/AMP). This may be related to the substrate-binding mechanism of Adk. It has been known that the catalytic mechanism of Adk is explained by “a random Bi-Bi mechanism”,⁴² where two substrate molecules bind to the corresponding binding sites at random. During the binding processes, each subdomain undergoes conformational change. A previous NMR study proposed that the conformational change occurring in one domain induced a concerted structural response to another domain to affect the second substrate-binding.⁴³ In other words, the two binding domains have cooperativity with respect to the substrate binding. Furthermore, Mg²⁺ directly interacts with the enzyme to affect the enzyme conformation, resulting in enhancement of the ligand binding and the overall catalytic activity, as well as the complex formation of Mg²⁺ with ADP. Because of these complicated factors, precise numerical analysis over the whole of ADP concentration region is impossible, although qualitative interpretation would be allowed.

In the absence of Mg²⁺, ADP has an occasion to be accommodated into both binding sites. The emission intensity profile (marked in red circles of Figure 8) shows a positive allosteric behavior, although the fitting by a typical allosteric binding model for the changes of monomer emission or

excimer emission was not successful because of the rather small cooperativity in the low ADP concentration region. A plausible reason is that the affinities of ADP toward the two binding sites are different and that the binding mode yielding larger association constants is not significantly associated with allosteric behavior.

In the presence of Mg^{2+} (10 mM), a two-phase profile became more distinct (marked in blue triangles of Figure 8). In the low ADP concentrations (<ca. 2.5 mM), the emission profile is similar to a simple Langmuir-type binding fashion. Calculated from the stability constant of $Mg^{2+} \bullet ADP = 2500 M^{-1}$,⁴⁴ more than 90% of ADP molecules exist as $ADP \cdot Mg^{2+}$ complex (denoted as $Mg^{2+} \bullet ADP$) under the ADP concentration region measured. The presence of Mg^{2+} facilitates the binding of ADP to the binding site in LID domain (the ATP-producing domain) in the same manner as the binding of a $ATP \cdot Mg^{2+}$ complex in the reversed reaction, whereas the association of $Mg^{2+} \bullet ADP$ to the binding site in AMP-bd domain (the AMP-producing domain) is very weak. This is suggested by the fact that the existence of excess Mg^{2+} inhibits the conversion of ADP into ATP/AMP because of a deficiency in the amount of Mg^{2+} -free ADP.⁴² Consequently, the simple 1:1 binding of $Mg^{2+} \bullet ADP$ becomes relatively dominant at the low ADP concentration region. In contrast, the amount of Mg^{2+} -free ADP molecules increases in the high ADP concentration region. In this case, the occupancy of the AMP-binding site by Mg^{2+} -free ADP gradually occurs. The full occupancy in the two binding sites increases the efficiency of conformational transition.

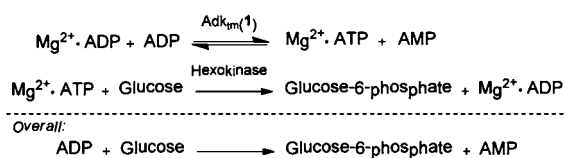
As described above, the observed emission spectral changes on the addition of ADP can be explained by the characteristics of the binding and conformational changes of the enzyme.

On addition of Mg^{2+} to the $ADP \cdot Adk_{tm}(1)$ complex, the increase in excimer emission intensity was observed (Figure S9). Since the excimer emission intensity is related with the extent of proximity of the two pyrene moieties, the effect of Mg^{2+} on the excimer emission intensity may suggest that the conformation becomes tighter during the phosphoryl transfer process.⁴⁵

Reversible and Repeatable Switching of Pyrene Emission Property Using Hexokinase-Coupled Reaction.

On the basis of the facts demonstrated above, switching of monomer/excimer emission of pyrene in the opposite direction, i.e., recovery of the OPEN form starting from the CLOSED form, was attempted by using a hexokinase-coupled reaction.³⁷ The whole reaction system is shown in Scheme 1.

Scheme 1. Whole Reaction Scheme for Recovery of OPEN Form of $Adk_{tm}(1)$



Since the conversion between ADP and ATP/AMP mediated by $Adk_{tm}(1)$ is reversible ($\Delta G^0 \sim 0$), the consumption of ATP by hexokinase is essential to shift the $Adk_{tm}(1)$ -mediated reaction to the forward direction. On the addition of Mg^{2+} and hexokinase to an enzyme solution showing the excimer emission by ADP binding, the intensity of emission band decreased with the recovery of the monomer emission over 100

min (Figure 9a). The spectral change is indicative of the conversion of ADP into ATP/AMP and the following hexokinase reaction.

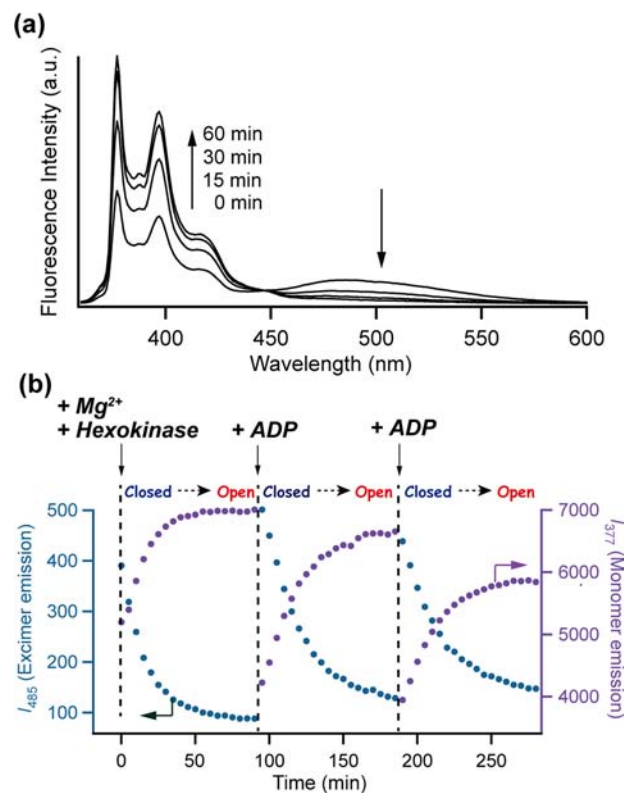


Figure 9. Recovery of monomer emission (OPEN form) and repeating experiment in 50 mM Tris-HCl, pH 7.5 at 25 °C, $[Adk_{tm}(1)] = 0.18 \mu M$, $[Glucose] = 10 \text{ mM}$, $[hexokinase] = 25 \text{ unit}$, $[MgCl_2] = 5 \text{ mM}$. (a) Observed emission spectral changes after addition of ADP (1 mM). (b) Emission intensity at 377 and 485 nm in a sequential addition of ADP (1 mM addition for each run).

Since excimer emission caused by ATP- or AMP-binding is very weak (see Figure S10), it can be concluded that the spectral change demonstrated in Figure 9a is mainly caused by the decrease in ADP. In other words, this spectral change indicates that $Adk_{tm}(1)$ released the reaction products (ATP and AMP) to reproduce the OPEN form and that the product release is surely associated with the conformational change to recover the OPEN form. Figure 9b demonstrates that a sequential addition of ADP affords the CLOSED form again. After the consumption of ADP, the second and third recoveries of the OPEN form were observed. The observed change in the emission intensity indicates the availability of the *one-pot* repeating emission switching.

CONCLUSION

The pyrene-conjugated Adk can function as a scaffold for the monomer/excimer emission switching system driven by the catalytic cycle of Adk (binding of a substrate, chemical process and release of a product). The appearance of the excimer emission under dilute conditions in aqueous media is remarkable because aggregation under highly concentrated conditions is, generally, the dominant factor to produce excimer emission in aqueous media. The spectral change is not a simple host-guest binding model but described by several kinds of

allosteric behaviors. This fact confirms that the observed spectral change is associated with the conformational transition of Adk. The switching of monomer/excimer emission is repeatable by a sequential addition of substrates in a one-pot, without any removal procedure for the substances in the solution. In this context, this can be regarded as an “in-situ chromic system”. The findings emerging in this work will contribute to the development of protein-based intelligent materials.

■ ASSOCIATED CONTENT

Supporting Information

Column chromatogram in the purification of Adk_{tm}(1), additional UV-vis and CD spectra, Adk activity assay. This material is available free of charge via the Internet at <http://pubs.acs.org>.

■ AUTHOR INFORMATION

Corresponding Author

*E-mail: tmatsuo@ms.naist.jp.

Notes

The authors declare no competing financial interest.

■ ACKNOWLEDGMENTS

We thank the financial supports from MEXT, Japan, The Green Photonics Project at NAIST provided by MEXT, Japan, and Innovations Inspired by Nature Research Program by Sekisui Integrated Research, Inc. The authors acknowledge Prof. Elisha Haas (Bar-Ilan University, Israel) for providing with the pEAK91 plasmid coding the adenylate kinase expression system and Mr. Leigh McDowell for kind advice during manuscript preparation.

■ REFERENCES

- (1) Wörsdörfer, B., Henning, L. M., Obexer, R., and Hilvert, D. (2012) Harnessing protein symmetry for enzyme design. *ACS Catal.* 2, 982–985.
- (2) Thomas, C. M., and Ward, T. R. (2005) Artificial metalloenzymes: proteins as hosts for enantioselective catalysis. *Chem. Soc. Rev.* 34, 337–346.
- (3) Steinreiber, J., and Ward, T. R. (2008) Artificial metalloenzymes as selective catalysts in aqueous media. *Coord. Chem. Rev.* 252, 751–766.
- (4) Gerstein, M., and Krebs, W. (1998) A database of macromolecular motions. *Nucleic Acids Res.* 26, 4280–4290.
- (5) Sawai, H., Yamanaka, M., Sugimoto, H., Shiro, Y., and Aono, S. (2012) Structural basis for the transcriptional regulation of heme homeostasis in *Lactococcus lactis*. *J. Biol. Chem.* 287, 30755–30768.
- (6) Woolley, G. A. (2005) Photocontrolling peptide α -helices. *Acc. Chem. Res.* 38, 486–493.
- (7) Panja, A., Matsuo, T., Nagao, S., and Hirota, S. (2011) DNA cleavage by the photocontrolled cooperation of Zn(II) centers in an azobenzene-linked dizinc complex. *Inorg. Chem.* 50, 11437–11445.
- (8) Suzuki, Y., Okuro, K., Takeuchi, T., and Aida, T. (2012) Friction-mediated dynamic disordering of phospholipid membrane by mechanical motions of photoresponsive molecular glue: Activation of ion permeation. *J. Am. Chem. Soc.* 134, 15273–15276.
- (9) Murphy, W. L., Dillmore, W. S., Modica, J., and Mrksich, M. (2007) Dynamic hydrogels: Translating a protein conformational change into macroscopic motion. *Angew. Chem., Int. Ed.* 46, 3066–3069.
- (10) Yuan, W. W., Yang, J. Y., Kopečková, P., and Kopeček, J. (2008) Smart Hydrogels containing adenylate kinase: Translating substrate recognition into macroscopic motion. *J. Am. Chem. Soc.* 130, 15760–15761.

(11) King, W. J., Pytel, N. J., Ng, K., and Murphy, W. L. (2010) Triggered drug release from dynamic microspheres via a protein conformational change. *Macromol. Biosci.* 10, 580–584.

(12) Sinev, M. A., Sineva, E. V., Ittah, V., and Haas, E. (1996) Domain closure in adenylate kinase. *Biochemistry* 35, 6425–6437.

(13) Shinmori, H., Furukawa, H., Fujimoto, K., Shimizu, H., Inouye, M., and Takeuchi, T. (2009) Characteristic fluorescence behavior of dialkynylpyrene derivatives in hydrophobic cavity of protein. *Chem. Lett.* 38, 84–85.

(14) Sinev, M., Landsmann, P., Sineva, E., Ittah, V., and Haas, E. (2000) Design consideration and probes for fluorescence resonance energy transfer studies. *Bioconjugate Chem.* 11, 352–362.

(15) Kajihara, D., Abe, R., Iijima, I., Komiyama, C., Sisido, M., and Hohsaka, T. (2006) FRET analysis of protein conformational change through position-specific incorporation of fluorescent amino acids. *Nat. Methods* 3, 923–929.

(16) Subach, O. M., Entenberg, D., Condeelis, J. S., and Verkhusha, V. V. (2012) A FRET-facilitated photoswitching using an orange fluorescent protein with the fast photoconversion kinetics. *J. Am. Chem. Soc.* 134, 14789–14799.

(17) Shimizu, H., Fujimoto, K., Furusyo, M., Maeda, H., Nanai, Y., Mizuno, K., and Inouye, M. (2007) Highly emissive π -conjugated alkynylpyrene oligomers: Their synthesis and photophysical properties. *J. Org. Chem.* 72, 1530–1533.

(18) Chen, S., Wang, L., Fahmi, N. E., Benkovic, S. J., and Hecht, S. M. (2012) Two pyrenylalanines in dihydrofolate reductase form an excimer enabling the study of protein dynamics. *J. Am. Chem. Soc.* 134, 18883–18885.

(19) Saintgiron, I., Gilles, A.-M., Margarita, D., Michelson, S., Monnot, M., Femandjian, S., Danchin, A., and Bârzu, O. (1987) Structural and catalytic characteristics of *Escherichia Coli* adenylate Kinase. *J. Biol. Chem.* 262, 622–629.

(20) Ensign, A. A., Jo, I., Yildirim, I., Krauss, T. D., and Bren, K. L. (2008) Zinc porphyrin: A fluorescent acceptor in studies of Zn-cytochrome c unfolding by fluorescence resonance energy transfer. *Proc. Natl. Acad. Sci. U.S.A.* 105, 10779–10784.

(21) Wieland, B., Tomasselli, A. G., Noda, L. H., Frank, R., and Schulz, G. E. (1984) The amino-acid-sequence of Gtp - Amp phosphotransferase from beef-heart Mitochondria - Extensive homology with cytosolic adenylate kinase. *Eur. J. Biochem.* 143, 331–339.

(22) Gerstein, M., Schulz, G., and Chothia, C. (1993) Domain closure in adenylate kinase - Joints on either side of 2 helices close like neighboring fingers. *J. Mol. Biol.* 229, 494–501.

(23) Müller, C. W., Schlauderer, G. J., Reinstein, J., and Schulz, G. E. (1996) Adenylate kinase motions during catalysis: An energetic counterweight balancing substrate binding. *Structure* 4, 147–156.

(24) Krishnamurthy, H., Lou, H. F., Kimple, A., Vieille, C., and Cukier, R. I. (2005) Associative mechanism for phosphoryl transfer: A molecular dynamics simulation of *Escherichia coli* adenylate kinase complexed with its substrates. *Proteins* 58, 88–100.

(25) Schulz, G. E., Müller, C. W., and Diederichs, K. (1990) Induced-fit movements in adenylate kinases. *J. Mol. Biol.* 213, 627–630.

(26) Müller, C. W., and Schulz, G. E. (1992) Structure of the complex between adenylate kinase from *Escherichia Coli* and the inhibitor Ap₅A refined at 1.9 Å resolution - A model for a catalytic transition state. *J. Mol. Biol.* 224, 159–177.

(27) Förster, T. (1969) Excimers. *Angew. Chem., Int. Ed. Engl.* 8, 333–343.

(28) Inouye, M., Fujimoto, K., Furusyo, M., and Nakazumi, H. (1999) Molecular recognition abilities of a new class of water-soluble cyclophanes capable of encompassing a neutral cavity. *J. Am. Chem. Soc.* 121, 1452–1458.

(29) Kano, K., Takenoshita, I., and Ogawa, T. (1982) γ -Cyclodextrin-enhanced excimer fluorescence of pyrene and effect of n-butyl alcohol. *Chem. Lett.* 1982, 321–324.

(30) Kano, K., Matsumoto, H., Hashimoto, S., Sisido, M., and Imanishi, Y. (1985) Chiral pyrene excimer in the γ -cyclodextrin cavity. *J. Am. Chem. Soc.* 107, 6117–6118.

(31) Ueno, A., Suzuki, I., and Osa, T. (1989) Association dimers, excimers, and inclusion complexes of pyrene-appended γ -cyclodextrins. *J. Am. Chem. Soc.* *111*, 6391–6397.

(32) Chang, K. C., Su, I. H., Senthilvelan, A., and Chung, W. S. (2007) Triazole-modified calix[4]crown as a novel fluorescent on-off switchable chemosensor. *Org. Lett.* *9*, 3363–3366.

(33) Hung, H. C., Cheng, C. W., Wang, Y. Y., Chen, Y. J., and Chung, W. S. (2009) Highly selective fluorescent sensors for Hg^{2+} and Ag^+ based on bis-triazole-coupled polyoxyethylenes in MeOH solution. *Eur. J. Org. Chem.*, 6360–6366.

(34) Senthilvelan, A., Ho, I. T., Chang, K. C., Lee, G. H., Liu, Y. H., and Chung, W. S. (2009) Cooperative recognition of a copper cation and anion by a calix[4]arene substituted at the lower rim by a β -amino- α , β -unsaturated ketone. *Chem.—Eur. J.* *15*, 6152–6160.

(35) Fujimoto, K., Muto, Y., and Inouye, M. (2005) A general and versatile molecular design for host molecules working in water: a duplex-based potassium sensor consisting of three functional regions. *Chem. Commun.*, 4780–4782.

(36) Bains, G. K., Kim, S. H., Sorin, E. J., and Narayanaswami, V. (2012) The extent of pyrene excimer fluorescence emission is a reflector of distance and flexibility: analysis of the segment linking the LDL receptor-binding and tetramerization domains of apolipoprotein E3. *Biochemistry* *51*, 6207–6219.

(37) Kunst, A., Draeger, B., and Ziegenhorn, J. (1984) UV-methods with hexokinase and glucose-6-phosphate dehydrogenase, in *Methods of Enzymatic Analysis* (Bergmeyer, H. U., Ed.) pp 163–172, Verlag Chemie, Weinheim, Germany.

(38) Jacob, M. H., Amir, D., Ratner, V., Gussakowsky, E., and Haas, E. (2005) Predicting reactivities of protein surface cysteines as part of a strategy for selective multiple labeling. *Biochemistry* *44*, 13664–13672.

(39) The names "ATP-producing site" and "AMP-producing site" mean that each site functions as a binding site for the corresponding compound in the reverse reaction ($\text{ATP} + \text{AMP} \rightarrow 2\text{ADP}$). Mg^{2+} enhances the binding constant of ADP by forming a substrate- Mg^{2+} -enzyme ternary complex. Tan, Y.-W., Hanson, J. A., and Yang, H. (2009) Direct Mg^{2+} binding activates adenylatekinase from *Escherichia coli*. *J. Biol. Chem.* *284*, 3306–3313.

(40) The fluorescence spectra for Ap_5A were measured in the presence of Mg^{2+} (5 mM), whereas the spectra shown in Figure 5 were taken without Mg^{2+} to avoid the conversion of ADP into ATP/AMP.

(41) Jencks, W. P. (1969) *Catalysis in Chemistry and Enzymology*, McGraw-Hill, New York.

(42) Sheng, X.-R., Li, X., and Pan, X.-M. (1999) An iso-random Bi Bi mechanism for adenylate kinase. *J. Biol. Chem.* *274*, 22238–22242.

(43) Ádén, J., and Wolf-Watz, M. (2007) NMR identification of transient complexes critical to adenylate kinase catalysis. *J. Am. Chem. Soc.* *129*, 14003–14012.

(44) Kuby, S., and Noltman, E. (1962) *The Enzymes*, Vol. 6, Academic Press, New York.

(45) Haas et al. has proposed the existence the substructures in the presence of substrates. See ref 14.